UDC 621.3.013 https://doi.org/10.20998/2074-272X.2025.2.07

B.I. Kuznetsov, T.B. Nikitina, I.V. Bovdui, K.V. Chunikhin, V.V. Kolomiets, B.B. Kobylianskyi

Method for reduction of magnetic field of uncertain extended technical objects based on their multyspheroidal model and compensating magnetic dipoles

***Problem**. The implementation of strict requirements for magnetic silence of elongated energy-saturated objects such as naval vessel and submarines is an important scientific and technical problem of magnetism of technical objects. **Purpose**. Development of method for reduction of magnetic field of uncertain extended technical objects based on their multyspheroidal model and optimization of parameters of compensating dipoles for compensate of spheroidal harmonics of external magnetic field of technical object. **Methodology.** Number, coordinates of spatial arrangement and magnitudes of spherical harmonics of compensating dipole of magnetic field sources calculated as magnetostatics geometric inverse problems solution in the form of nonlinear minimax optimization problem based on multyspheroidal model of magnetic field of extended technical objects. Nonlinear objective function calculated as the weighted sum of squared of resulting magnetic field COMSOL Multiphysics software package used. Nonlinear minimax optimization problems solutions calculated based on particle swarm nonlinear optimization algorithms. **Results.** The results of reduction of the initial magnetic field of extended technical objects based on their multyspheroidal model and optimization of parameters of compensating magnetic dipoles for compensate of spheroidal harmonics of external magnetic field of technical object using multyspheroidal model of the magnetic field in the form of spatial prolate spheroidal harmonics in the prolate spheroidal coordinate system and taking into account the uncertainty of the magnetic characteristics of extended technical objects. **Originality.** For the first time the method for reduction of magnetic field of uncertain extended technical objects based on their multyspheroidal model and optimization of parameters of compensating magnetic dipoles for compensate of spheroidal harmonics of external magnetic field of technical object using multyspheroidal model of the magnetic field developed. Unlike known methods, the developed method makes it possible to increase the efficiency of magnetic field reduction of uncertain extended technical objects. **Practical value.** It is theoretically shown the possibility to reduce by almost 100 times of modulus of induction and horizontal component of the induction of the original magnetic field of uncertain extended technical objects based on optimization of parameters of compensating magnetic dipoles for compensate of spheroidal harmonics of external magnetic field of technical object using multyspheroidal model of the magnetic field.* References 48, figures 6.

Key words: **extended technical objects, magnetic field, multyspheroidal model, magnetic silencing, prolate spheroidal coordinate system, spatial prolate spheroidal harmonics, control, uncertainty.**

***Проблема.** Реалізація жорстких вимог щодо магнітної тиші витягнутих енергонасичених об'єктів, таких як військові кораблі та підводні човни, є важливою науковою та технічною проблемою магнетизму технічних об'єктів. **Мета.** Розробка методу зменшення магнітного поля невизначених протяжних технічних об'єктів на основі їх мультисфероїдальної моделі і оптимізації параметрів компенсуючих магнітних диполів для компенсації сфероїдальних гармонік зовнішнього магнітного поля технічного об'єкта. **Методологія.** Параметри компенсуючих дипольних джерел магнітного поля розраховані як рішення обернених геометричних задач магнітостатики у формі нелінійної задачі мінімаксної оптимізації на основі мультисфероїдальної моделі магнітного поля витягнутих технічних об'єктів. Нелінійна цільова функція розрахована як зважена сума квадратів результуючого магнітного поля з використанням програмного пакету COMSOL Multiphysics. Розв'язки задач нелінійної мінімаксної оптимізації розраховані на основі алгоритмів нелінійної оптимізації роєм частинок. **Результати.** Результати компенсації вихідного магнітного поля витягнутих технічних об'єктів на основі їх мультісфероїдальної моделі і оптимізації параметрів компенсуючих магнітних диполів для компенсації сфероїдальних гармонік зовнішнього магнітного поля технічного об'єкта з використанням мультисфероїдальної моделі магнітного поля в вигляді просторових витягнутих сфероїдальних гармонік в витягнутій сфероїдній системі координат та з врахуванням невизначеності магнітних характеристик витягнутих технічних об'єктів. **Оригінальність**. Вперше розроблено метод зменшення магнітного поля невизначених протяжних технічних об'єктів на основі їх мультісфероїдальної моделі і оптимізації параметрів компенсуючих магнітних диполів для компенсації сфероїдальних гармонік зовнішнього магнітного поля технічного об'єкта з використанням мультисфероїдальної моделі магнітного поля . На відміну від відомих методів, розроблений метод дозволяє підвищити ефективність зменшення магнітного поля невизначених протяжних технічних об'єктів. **Практична цінність**. Показана теоретична можливість зменшення майже в 100 разів модуля індукції та горизонтальної складової індукції вихідного магнітного поля невизначених протяжних технічних об'єктів на основі оптимізації параметрів компенсуючих магнітних диполів для компенсації сфероїдальних гармонік зовнішнього магнітного поля. поля технічного об'єкта з використанням мультисфероїдальної моделі магнітного поля.* Бібл. 48, рис. 6.

Ключові слова: **витягнуті технічні об'єкти, магнітне поле, мультисфероїдальна модель, магнітна тиша, витягнута сфероїдна система координат, просторові витягнуті сфероїдні гармоніки, управління, невизначеність.**

Introduction. Strict requirements are imposed on the accuracy of the description of the magnetic field near a technical object in shipboard magnetism such as naval vessel and submarines, when solving problems of electromagnetic compatibility, as well as in developing means of magnetic orientation and ensuring the magnetic cleanliness of spacecraft [1–3]. The main threat to naval vessel and submarines in modern naval warfare are naval mines. The magnetic protection complex of naval vessel and submarines from naval mines designed to reduce the magnetic field level at the control depth at which mine fuses do not operate through the following channels: magnetic, responding to the magnetic induction of a constant and slowly changing of magnetic field induction, responding to changes in the induction of a constant and slowly changing magnetic field during the movement of the naval vessel and submarines, electromagnetic, responding to the low-frequency electromagnetic field of the naval vessel and submarines [4–8].

The requirements for magnetic protection of naval vessel and submarines formulated as follows: the maximum value of the magnetic induction module of a constant and slowly changing magnetic field calculated from the magnetic signature (pass-through characteristic) of the naval vessel and submarines at the control depth, should not exceed the specified value; the maximum value of the change in the horizontal component of the magnetic induction of a constant and slowly magnetic field changing over a certain period of time, calculated from the magnetic signature of the naval vessel and submarines, at the control depth when it moves at the nominal speed, should not exceed the specified value; the maximum value of the magnetic induction module of the low-frequency magnetic field of 50 Hz, calculated from the magnetic signature of the naval vessel and submarines at the control depth should not exceed the specified value.

To meet these stringent requirements for magnetic silence, all ships periodically carry out the demagnetization (degaussing) process on special magnetodynamic stands. To enhance the demagnetization process, a special solenoidal winding is installed on the ship's hull. To compensate the magnetic field of naval vessel and submarines a system of compensation windings are used in three orthogonal coordinates associated with the ship – in the longitudinal, transverse and vertical directions [4–7]. Compensation of the magnetic field of the main magnetization of the ship in the vertical direction is carried out using main parallel coils designed to compensate for the large magnetizations of the bow and stern of the ship. In addition to the general ship compensation windings, separate local electromagnetic compensators are also used.

Naval vessel and submarines are elongated energy-saturated objects and have a cigar-shaped appearance. The use of a spherical expansion of the scalar potential for objects with a predominant overall size does not make it possible to describe the magnetic field near their surface [9–13]. It seems relevant at present to use of spatial harmonic analysis in an extended spheroidal coordinate system, where the shape of the coordinate surfaces makes it possible to bring the description area closer to the surface of the object itself [14–16].

To compensate of initial magnetic field generated by these energy-saturated elongated object, it is theoretically possible to use compensating spheroidal magnetic field sources located at points in the space of the technical object, calculated when designing a multyspheroidal model of the original magnetic field of the technical object.

Multyspheroidal sources of the magnetic field should be taken equal in magnitude, but opposite in sign to the corresponding spheroidal harmonics of the spheroidal sources of the original magnetic field of the technical object. However, the technical implementation of such compensating spheroid magnetic field sources presents certain difficulties [16]. Therefore, we will consider the generation of a compensating magnetic field using compensating dipole magnetic field sources.

In various operating modes of an energy-saturated elongated technical object, as well as during operation, its signature changes, therefore, when reducing it, it is necessary to take into account the uncertainties of the magnetic signature of a technical object [17–19].

Optimization of parameters of compensating dipoles based on multyspheroidal model of magnetic field of energy-saturated elongated objects will improve the efficiency of reduction of original magnetic field of such uncertain objects.

The purpose of the work is to develop a method for reduction of magnetic field of uncertain extended technical objects based on their multyspheroidal model and optimization of parameters of compensating dipoles for compensate of spheroidal harmonics of external magnetic field of technical object.

Definition of forward multyspheroidal magnetostatics problem. Let's consider a multyspheroidal model of the original magnetic field of an energy-saturated extended technical object in an elongated spheroidal coordinate system. Let us assume that the initial magnetic field of an extended energy-saturated object is generated using I spheroidal magnetic field sources located at points in space of the technical object with coordinates (x_i,y_i, z_i) in a rectangular coordinate system associated with the center of the technical object as shown in Fig. 1.

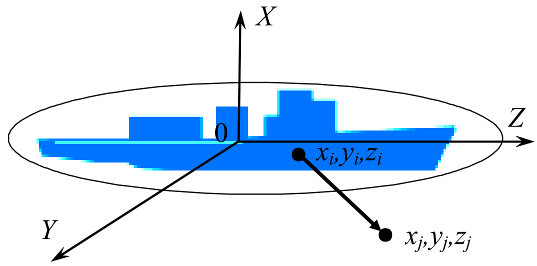

Fig. 1. Energy-saturated extended technical object

Then the components $H_{\xi ij}$, $H_{\eta ij}$, $H_{\varphi ij}$ of the magnetic field generated by these I spheroidal sources at J measurement points are calculated at points with coordinates ξ_{ij}, η_{ij}, φ_{ij} in elongated spheroidal coordinate systems associated with the centers of these sources, according to the following dependencies [16]

$$H_{\xi ij} = -\frac{\sqrt{\xi_{ij}^2-1}}{c_i\sqrt{\xi_{ij}^2-\eta_{ij}^2}} \sum_{n=1}^{\infty}\sum_{m=0}^{n} \frac{dQ_{ni}^m(\xi_{ij})}{d\xi_{ij}} \left\{c_{ni}^m \cos(m\varphi_{ij}) + s_{ni}^m \sin(m\varphi_{ij})\right\} P_{ni}^m\left(\cos(\eta_{ij})\right),$$

$$H_{\eta ij} = -\frac{\sqrt{1-\eta_{ij}^2}}{c_i\sqrt{\xi_{ij}^2-\eta_{ij}^2}} \sum_{n=1}^{\infty}\sum_{m=0}^{n} Q_{ni}^m(\xi_{ij}) \frac{dP_{ni}^m\left(\cos(\eta_{ij})\right)}{d\eta_{ij}} \left\{c_{ni}^m \cos(m\varphi_{ij}) + s_{ni}^m \sin(m\varphi_{ij})\right\}, \quad (1)$$

$$H_{\varphi ij} = \frac{m}{c_i\sqrt{\left(\xi_{ij}^2-1\right)\left(1-\eta_{ij}^2\right)}} \sum_{n=1}^{\infty}\sum_{m=0}^{n} Q_{ni}^m(\xi) P_{ni}^m\left(\cos(\eta_{ij})\right)\left\{c_{ni}^m \sin(m\varphi_{ij}) - s_{ni}^m \cos(m\varphi_{ij})\right\},$$

here are the spheroidal coordinates ξ_{ij}, η_{ij}, φ_{ij} of observation points of the space of a technical object with coordinates (x_j, y_j, z_j) in rectangular coordinate systems associated with the center of the technical object, from the location points of spheroidal magnetic field sources with coordinates (x_i, y_i, z_i) in an orthogonal system coordinates associated with the center of the technical object are related by the relation

$$
\left.
\begin{aligned}
x_j - x_i &= c_i \cdot \sqrt{\xi_{ij}^2 - 1} \cdot \sqrt{1 - \eta_{ij}^2} \cdot \cos(\varphi_{ij}); \\
y_j - y_i &= c_i \cdot \sqrt{\xi_{ij}^2 - 1} \cdot \sqrt{1 - \eta_{ij}^2} \cdot \sin(\varphi_{ij}); \\
z_j - z_i &= c_i \cdot \xi_{ij} \cdot \eta_{ij};
\end{aligned}
\right\} \Rightarrow
\begin{aligned}
&\xi_{ij} \in [1, \infty[; \\
&\eta_{ij} \in [0,1]; \\
&\varphi_{ij} \in [0, 2\pi];
\end{aligned}
\tag{2}
$$

where $P_{ni}^m(\xi_{ij})$, $Q_{ni}^m(\xi_{ij})$ associated Legendre functions of the first and second kind, respectively, with degree n and order m; c_i, c_{ni}^m, s_{ni}^m – constant coefficients characterizing the amplitudes of external spheroidal harmonics of the magnetic field.

Measurements and calculations of magnetic field components it is more convenient to carry out in the orthogonal coordinate system (x_j, y_j, z_j), the transition to which for the components H_{xij}, H_{yij}, H_{zij} is carried out using the formulas [16]:

$$
\begin{aligned}
H_{xij} &= \xi_{ij} \cdot \frac{\sqrt{1-\eta_{ij}^2}}{\sqrt{\xi_{ij}^2 - \eta_{ij}^2}} \cdot \cos(\varphi_{ij}) \cdot H_{\xi ij} - \eta_{ij} \cdot \frac{\sqrt{\xi_{ij}^2 - 1}}{\sqrt{\xi_{ij}^2 - \eta_{ij}^2}} \cdot \cos(\varphi_{ij}) \cdot H_{\eta ij} - \sin(\varphi_{ij}) \cdot H_{\varphi ij} \\
H_{yij} &= \xi_{ij} \cdot \frac{\sqrt{1-\eta_{ij}^2}}{\sqrt{\xi_{ij}^2 - \eta_{ij}^2}} \cdot \sin(\varphi_{ij}) \cdot H_{\xi ij} - \eta_{ij} \cdot \frac{\sqrt{\xi_{ij}^2 - 1}}{\sqrt{\xi_{ij}^2 - \eta_{ij}^2}} \cdot \sin(\varphi_{ij}) \cdot H_{\eta ij} + \cos(\varphi_{ij}) \cdot H_{\varphi ij}, \\
H_{zij} &= \eta_{ij} \cdot \frac{\sqrt{\xi_{ij}^2 - 1}}{\sqrt{\xi_{ij}^2 - \eta_{ij}^2}} \cdot H_{\xi ij} + \xi_{ij} \cdot \frac{\sqrt{1-\eta_{ij}^2}}{\sqrt{\xi_{ij}^2 - \eta_{ij}^2}} \cdot H_{\eta ij}
\end{aligned}
\tag{3}
$$

Harmonic analysis in elongated spheroidal coordinate system based on (1) or (3) requires the calculation of associated Legendre polynomials of the first $P_{ni}^m(\xi_{ij})$ and second $Q_{ni}^m(\xi_{ij})$ kind. Polynomials $Q_{ni}^m(\xi_{ij})$ of the second kind calculated using the well-known formula with a limitation on the number of terms of the infinite series [18]

$$
Q_{ni}^m(\xi_{ij}) = \frac{(-1)^m \cdot (2)^{m-1} \cdot (\xi_{ij}^2 - 1)^{\frac{m}{2}}}{\xi_{ij}^{n+m+1}} \times \sum_{k=0}^{\infty} \frac{\Gamma_i\left(\frac{n}{2} + \frac{m}{2} + k + \frac{1}{2}\right) \cdot \Gamma_i\left(\frac{n}{2} + \frac{m}{2} + k + 1\right)}{\Gamma_i(k+1) \cdot \Gamma_i\left(n + k + \frac{3}{2}\right) \cdot \xi_{ij}^{2k}}. \tag{4}
$$

The region $\xi \in [\xi_o, 4]$ places strict demands on the accuracy of $Q_{ni}^m(\xi_{ij})$ function calculations. Algorithms for direct calculation $Q_{ni}^m(\xi_{ij})$ obtained in the form of finite sums [16]

$$
\begin{aligned}
Q_{ni}^m(\xi_{ij}) &= \frac{P_{ni}(\xi_{ij})}{2} \cdot \ln\left(\frac{\xi_{ij}+1}{\xi_{ij}-1}\right) - \sum_{k=1}^{n} \frac{1}{k} \cdot \sum_{\lambda=0}^{m} C_{mi}^{\lambda} \cdot P_{k-1}^{\lambda}(\xi_{ij}) \cdot P_{n-k}^{m-\lambda}(\xi_{ij}) + \frac{(1 - \delta(m,0))}{2} \times \ldots \\
&\ldots \times \sum_{q=0}^{m-1} C_{mi}^{q} \cdot P_{ni}^{q}(\xi_{ij}) \cdot (m-q-1)! \cdot \frac{(\xi_{ij}-1)^{m-q} - (\xi_{ij}+1)^{m-q}}{(-1)^{m-q-1}(\xi_{ij}^2 - 1)^{\frac{m-q}{2}}};
\end{aligned}
$$

$$
Q_{ni}^m(\xi_{ij}) = \frac{(\xi_{ij}^2 - 1)^{\frac{m}{2}} n! m!}{2^{n+1}} \sum_{k=0}^{m} \frac{(k+n)! \, \Omega(m-k, \xi_{ij})}{k!(m-k)!} \sum_{\lambda=k}^{n} \frac{(\xi_{ij}-1)^{n-\lambda} (\xi_{ij}+1)^{\lambda-k}}{\lambda!(n+k-\lambda)!(\lambda-k)!(n-\lambda)!} - \sum_{k=1}^{n} \frac{1}{k} \sum_{\lambda=0}^{m} C_{mi}^{\lambda} P_{k-1}^{\lambda}(\xi_{ij}) P_{n-k,i}^{m-\lambda}(\xi_{ij});
$$

$$
\Omega(\nu, \xi_{ij}) = \left\{
\begin{aligned}
&\nu = 0 \quad \ln\left(\frac{\xi_{ij}+1}{\xi_{ij}-1}\right) \\
&\nu \neq 0 \quad (-1)^{\nu-1}(\nu-1)! \frac{(\xi_{ij}-1)^{\nu} - (\xi_{ij}+1)^{\nu}}{(\xi_{ij}^2-1)^{\nu}}
\end{aligned}
\right\}, \quad C_n^k = \frac{n!}{(n-k)! \, k!}. \tag{5}
$$

Note that the calculation of the components $H_{\xi ij}$, $H_{\eta ij}$, $H_{\varphi ij}$ of the magnetic field in spheroidal coordinates ξ_{ij}, η_{ij}, φ_{ij} using (1) or components H_{xij}, H_{yij}, H_{zij} in the orthogonal coordinate system (x_j, y_j, z_j) using (3) generated by spheroidal sources of the magnetic field for given values of parameters c_i and spatial spheroidal harmonics c_{ni}^m, s_{ni}^m at measurement points with coordinates (x_j, y_j, z_j) is a forward problem of magnetostatics for spheroidal magnetic field sources [20–25].

Definition of forward multydipole magnetostatics problem. To compensate for the spheroidal spatial harmonics of magnetic field of an energy-saturated extended object, we introduce C dipole magnetic field sources located at the C points of space of the technical object with coordinates (x_c, y_c, z_c) in a rectangular coordinate system associated with the center of the technical object. Let us define the spherical harmonics g_{nc}^m, h_{nc}^m of these C compensating dipole magnetic field sources.

Let us consider the calculation of the components of the magnetic field generated by these C dipole magnetic field sources at the magnetic field measurement points with coordinates (x_j, y_j, z_j) in a rectangular coordinate system associated with the center of the technical object. Let us calculate the spherical angular coordinates r_{cj}, φ_{cj}, θ_{cj} under which the measurement points with coordinates (x_j, y_j, z_j) are «visible» from the location points of dipole magnetic field sources with coordinates(x_c, y_c, z_c) in a rectangular coordinate system, associated with the center of the technical object, from the following relationships

$$\begin{aligned} x_j - x_c &= r_{cj} \cdot \sin(\theta_{cj})\cos(\varphi_{cj}); & r_{cj} &\in [0,\infty[\\ y_j - y_c &= r_{cj} \cdot \sin(\theta_{cj}) \cdot \sin(\varphi_{cj}); \Rightarrow & \theta_{cj} &\in [0,\pi] \\ z_j - z_c &= r_{cj} \cdot \cos(\theta_{cj}). & \varphi_{cj} &\in [0,2\pi] \end{aligned} \quad (6)$$

Then the components H_{rcj}, $H_{\varphi cj}$, $H_{\theta cj}$ of the magnetic field in the spherical coordinate system r_{cj}, φ_{cj}, θ_{cj} associated with the center of location of the compensating dipole source of the magnetic field, are calculated using the following formulas [20]

$$\begin{aligned} H_{rcj} &= \sum_{n=1}^{\infty}\sum_{m=0}^{n} \frac{n+1}{r^{n+2}} \left\{ g_{nc}^m \cos(m\varphi_{cj}) + h_{nc}^m \sin(m\varphi_{cj}) \right\} \cdot P_{nc}^m\left(\cos(\theta_{cj})\right); \\ H_{\theta cj} &= -\sum_{n=1}^{\infty}\sum_{m=0}^{n} \frac{1}{r^{n+2}} \left\{ g_{nc}^m \cos(m\varphi_{cj}) + h_{nc}^m \sin(m\varphi_{cj}) \right\} \frac{dP_{nc}^m\left(\cos(\theta_{cj})\right)}{d\theta_{cj}}; \\ H_{\varphi cj} &= \sum_{n=1}^{\infty}\sum_{m=0}^{n} \frac{m}{r^{n+2}} \left\{ g_{nc}^m \sin(m\varphi_{cj}) - h_{nc}^m \cos(m\varphi_{cj}) \right\} \frac{P_{nc}^m\left(\cos(\theta_{cj})\right)}{\sin(\theta_{cj})}. \end{aligned} \quad (7)$$

Using the calculated components H_{rcj}, $H_{\varphi cj}$, $H_{\theta cj}$ of the magnetic field in the spherical coordinate system r_{cj}, φ_{cj}, θ_{cj} we calculate the components H_{xcj}, H_{ycj}, H_{zcj} of magnetic field with orthogonal coordinate system, associated with the center of the compensating dipole magnetic field source according to the following formulas [20]

$$\begin{aligned} H_{xcj} &= H_{rcj} \sin(\theta_{cj})\cos(\varphi_{cj}) + H_{\theta cj}\cos(\theta_{cj})\cos(\varphi_{cj}) - H_{\varphi cj}\sin(\varphi_{cj}); \\ H_{ycj} &= H_{rcj} \sin(\theta_{cj})\sin(\varphi_{cj}) + H_{\theta cj}\cos(\theta_{cj})\sin(\varphi_{cj}) + H_{\varphi cj}\cos(\varphi_{cj}); \\ H_{zcj} &= H_{rcj}\cos(\theta_{cj}) - H_{0cj}\sin(\theta_{cj}). \end{aligned} \quad (8)$$

Let us take the axes of the orthogonal coordinate systems of compensating dipole sources parallel to the corresponding axes of the orthogonal coordinate system associated with the center of the technical object. Then the magnetic field components H_{xc}, H_{yc}, H_{zc} in an orthogonal coordinate system associated with the center of a technical object generated by all compensating dipole sources of magnetic field in currents, measurements with coordinates (x_j, y_j, z_j) are calculated as sums of the corresponding components H_{xcj}, H_{ycj}, H_{zcj} of magnetic field generated by individual compensating dipole sources at measurement points with coordinates (x_j, y_j, z_j).

Note that the calculation of the components H_{rcj}, $H_{\varphi cj}$, $H_{\theta cj}$ of the magnetic field in the spherical coordinate system r_{cj}, φ_{cj}, θ_{cj} using (1) or components H_{xcj}, H_{ycj}, H_{zcj} of magnetic field with orthogonal coordinate system (x_j, y_j, z_j) using (3) generated by spherical sources of the magnetic field for given values of spherical harmonics g_{nc}^m, h_{nc}^m at measurement points with coordinates (x_j, y_j, z_j) is a forward problem of magnetostatics for spherical magnetic field sources [26–30].

Definition of prediction geometric inverse problems of magnetostatics. Let us now consider the definition of the prediction geometric inverse problems of magnetostatics based on a forward multyspheroidal model (1) of the initial magnetic field of an energy-saturated extended object [26–34]. As a result of solving the prediction of the geometric inverse problem of magnetostatics based on the multyspheroidal model (1) of the original magnetic field of the energy-saturated extended control object, it is necessary to calculate the following coordinates (x_i, y_i, z_i) of the location of the multyspheroidal sources of the original magnetic field in the space of the technical object and the parameters c_i and spatial spheroidal harmonics c_{ni}^m, s_{ni}^m in such a way that, based on this mathematical model (1), the values of the magnetic field at measurement points with coordinates (x_j, y_j, z_j) are close to the experimentally measured values of the magnetic field in these measuring points.

A feature of the energy-saturated extended technical objects are the uncertainty of the magnetic characteristics of their elements and their change in different operating modes [35–40]. Let us introduce the vector $\boldsymbol{G}$ of uncertainties of the parameters of the magnetic characteristics of energy-saturated extended technical object [41–44].

Let us introduce the vector $\boldsymbol{Y_M}(\boldsymbol{G})$ of the measured values of the magnetic field signature of a technical object, the components of which are the measured components $H_{xk}(\boldsymbol{G})$, $H_{yk}(\boldsymbol{G})$, $H_{zk}(\boldsymbol{G})$ of the magnetic field of the technical object for given rectangular coordinates (x_j, y_j, z_j) associated with the center of the technical object. Note that the vector $\boldsymbol{Y_M}(\boldsymbol{G})$ of measured values of the magnetic field signature of a technical object depends on the operating modes of the technical object and on the vector $\boldsymbol{G}$ of uncertainties of the parameters of the magnetic cleanliness of the energy-saturated extended technical object units.

Let us introduce the vector $\boldsymbol{X}$ of the desired parameters of solving the prediction of the geometric inverse problem of magnetostatics, the components of which are the coordinates (x_i, y_i, z_i) of the location of spheroidal sources of the magnetic field at points in the space of a technical object in a rectangular coordinate system associated with the center of the technical object and given magnitudes of parameters c_i and spatial spheroidal harmonics c_{ni}^m, s_{ni}^m of these spheroidal magnetic field sources.

Then for given coordinate values (x_i, y_i, z_i) of the location of spheroidal magnetic field sources, at points in space of a technical object in a rectangular coordinate system associated with the center of the technical object and given values of parameters c_i and spatial spheroidal harmonics c_{ni}^m, s_{ni}^m components $H_{xkn}(\boldsymbol{X},\boldsymbol{G})$, $H_{ykn}(\boldsymbol{X},\boldsymbol{G})$, $H_{zkn}(\boldsymbol{X},\boldsymbol{G})$ H_{xij}, H_{yij}, H_{zij} of the magnetic field generated by these spheroidal magnetic field sources at measurement points with coordinates (x_i, y_i, z_i) in a rectangular coordinate system associated with the center of the technical object can be calculated based on forward multyspheroidal magnetic field model (1).

The values of parameters c_i and spatial spheroidal harmonics c_{ni}^m, s_{ni}^m of forward multyspheroidal magnetic field model (1) of an elongated energy-saturated object in an elongated spheroidal coordinate system ξ, η, φ depended on the operating modes of the energy-saturated extended technical object and, therefore, are functions of the components of the vector $\boldsymbol{G}$ of uncertainties of the parameters of the magnetic cleanliness of the energy-saturated extended technical object.

Therefore the components $\boldsymbol{H_{xkn}}(\boldsymbol{X},\boldsymbol{G})$, $\boldsymbol{H_{ykn}}(\boldsymbol{X},\boldsymbol{G})$, $\boldsymbol{H_{zkn}}(\boldsymbol{X},\boldsymbol{G})$, $\boldsymbol{H_{xij}}$, $\boldsymbol{H_{yij}}$, $\boldsymbol{H_{zij}}$ of the magnetic field generated by these spheroidal magnetic field sources at measurement points with coordinates (x_j, y_j, z_j) are also functions of the vector $\boldsymbol{G}$ of uncertainties of the parameters of the magnetic cleanliness of the energy-saturated extended technical object and the vector $\boldsymbol{X}$ of the desired parameters of solving the prediction of the geometric inverse problem of magnetostatics.

Let us introduce the vector $\boldsymbol{Y_C}(\boldsymbol{X},\boldsymbol{G})$ of calculated values of the magnetic field signature of a technical object, the components of which $\boldsymbol{H_{xkn}}(\boldsymbol{X},\boldsymbol{G})$, $\boldsymbol{H_{ykn}}(\boldsymbol{X},\boldsymbol{G})$, $\boldsymbol{H_{zkn}}(\boldsymbol{X},\boldsymbol{G})$, $\boldsymbol{H_{xij}}$, $\boldsymbol{H_{yij}}$, $\boldsymbol{H_{zij}}$ are calculated values components of the magnetic field of a technical object for given measurement points with coordinates (x_j, y_j, z_j) in a rectangular coordinate system associated with the center of the technical object.

Let us introduce the $\boldsymbol{E}(\boldsymbol{X},\boldsymbol{G})$ vector of the discrepancy between the vector $\boldsymbol{Y_M}(\boldsymbol{G})$ of the measured magnetic field and the vector $\boldsymbol{Y_C}(\boldsymbol{X},\boldsymbol{G})$ of the predicted by model (3) magnetic field

$$\boldsymbol{E}(\boldsymbol{X},\boldsymbol{G}) = \boldsymbol{Y_M}(\boldsymbol{G}) - \boldsymbol{Y_C}(\boldsymbol{X},\boldsymbol{G}) . \qquad (9)$$

Then the solution of prediction geometric inverse problem of magnetostatics comes down to the standard approach of designing a robust prediction multyspheroidal model of magnetic field of an energy-saturated extended object, when the coordinates (x_i, y_i, z_i) of the location of spheroidal sources of the magnetic field at points in the space of a technical object in a rectangular coordinate system associated with the center of the technical object and magnitudes of parameters c_i and spatial spheroidal harmonics c_{ni}^m, s_{ni}^m of these spheroidal magnetic field sources are found from the conditions for minimizing the vector of the discrepancy between the vector of the measured magnetic field and the vector of the predicted by forward multyspheroidal model magnetic field, but for the «worst» the vector $\boldsymbol{G}$ of uncertainties of the parameters of the magnetic characteristics of energy-saturated extended technical object are found from the conditions for maximizing the same vector of the discrepancy between the vector of the measured magnetic field and the vector of the predicted by multyspheroidal model of magnetic field.

Definition of control geometric inverse problems of magnetostatics. Let us now consider the definition of control geometric inverse problem of magnetostatics based on a multydipole model (1) of the compensating magnetic field of an energy-saturated extended control object. As a result of solving the control of the geometric inverse problem of magnetostatics on the basis of a multy-dipole model (7) of the compensating magnetic field of an energy-saturated extended control object, it is necessary to calculate the coordinates (x_c, y_c, z_c) of the location C of multy-dipole sources of the compensating magnetic field in the space of energy-saturated extended control object and the magnitude g_{nc}^m, h_{nc}^m of their spherical spatial harmonics, in such a way that, on the basis of this, the control of the mathematical model (7) of components values $\boldsymbol{H_{xc}}$, $\boldsymbol{H_{yc}}$, $\boldsymbol{H_{zc}}$ of magnetic field at the measurement points with coordinates (x_j, y_j, z_j) were close in magnitude but oppositely directed to the values of the initial magnetic field calculated on the basis of the predictions of the multyspheroidal model (1) at the same J measurement points with coordinates (x_j, y_j, z_j).

Let us introduce the vector $\boldsymbol{X}$ of the desired parameters for solving the problem of compensating of initial magnetic field of energy-saturated extended control object, whose components are unknown values of coordinates (x_i, y_i, z_i) of the location of spherical sources of the compensating magnetic field at points in the space of a technical object in a rectangular coordinate system associated with the center of the technical object and unknown values magnitude g_{nc}^m, h_{nc}^m of their spherical spatial harmonics of magnetic field of these spherical compensating sources.

Then, for a given value of the vector $\boldsymbol{X}$ of the desired parameters of the compensating dipoles, based on (7), the vector $\boldsymbol{B_c}(\boldsymbol{X})$ of the compensating magnetic field generated by all compensating dipoles at the specified points in space, in particular at the control depth of a technical object generated by all compensating dipoles can be calculated.

Then we calculated the vector $\boldsymbol{B_R}(\boldsymbol{X},\boldsymbol{G})$ of resulting magnetic field at the specified points in space, in particular at the control depth of a technical object generated by energy-saturated extended control object and all compensating elements

$$\boldsymbol{B}_R(\boldsymbol{X},\boldsymbol{G})=\boldsymbol{B}(\boldsymbol{G})+\boldsymbol{B}_c(\boldsymbol{X}). \qquad (10)$$

Then the problem of calculated unknown values of vector $\boldsymbol{X}$ of the desired parameters for solving the problem of compensating of initial magnetic field of energy-saturated extended control object, whose components are unknown values of coordinates (x_i, y_i, z_i) of the location of spherical sources of the compensating magnetic field at points in the space of a technical object in a rectangular coordinate system associated with the center of the technical object and unknown values magnitude g_{nc}^{m}, h_{nc}^{m} of their spherical spatial harmonics of magnetic field of these spherical compensating sources can be reduced to solving the problem of minimax optimization of resulting magnetic field (10) generated by energy-saturated extended control object and all compensating elements at the specified points in space, in particular at the control depth of a technical object.

This approach is also standard when designing of robust control by resulting magnetic field of an energy-saturated extended control object, when the coordinates of the spatial arrangement and the magnitudes of the compensating dipole calculated from the conditions for minimizing modulus of spacecraft resulting magnetic field (10) at the specified points in space, in particular at the control depth of a technical object, but for the «worst» values of the vector of uncertainty parameters of the energy-saturated extended technical object magnetic characteristics.

Inverse problems solution method. Components of the vector games (9), (10) are nonlinear functions of the vector $\boldsymbol{X}$ of required parameters and the vector $\boldsymbol{G}$ of uncertainty parameters of geometric inverse magnetostatics problem for prediction and control by magnetic signature of an energy-saturated extended object based on a multydipole model (1) taking into account forward problem uncertainties and calculated by COMSOL Multiphysics software.

A feature of the calculated solution problem is the multy-extremal nature of games payoff (9), (10) so that the considered region of possible solutions contains local minima and maxima. This due to fact that when minimizing the resulting magnetic field at one point in the signature of technical object, the magnetic field level at another point in signature of this technical object increases due to under compensation or overcompensation of the original magnetic field of technical object. Therefore, to calculate the solution this vector games (8) – (10) used stochastic multy-agent optimization algorithms [45].

To adapt the PSO method in relation to the problem of finding Pareto-optimal solutions on the set of possible values of a vector criterion, it is most simple to use binary preference relations that determine the Pareto dominance of individual solutions. To find a unique solution of a vector games (9), (10) from a set of Pareto-optimal solutions used information about the binary relationships of preferences of local solutions relative to each other [45]. To calculate one single global solution to the vector games (9), (10) individual swarms exchange information with each other during the calculation of optimal solutions to local games. Information about the global optimum obtained by particles from another swarm used to calculate the speed of movement of particles from another swarm, which allows calculated all Pareto-optimal solutions. To increase the speed of finding a global solution, special nonlinear algorithms of stochastic multy-agent optimization in which the motion of i particle of j swarm described by the following expressions [46]

$$\begin{aligned} v_{ij}(t+1) &= w_{1j}v_{ij}(t)+c_{1j}r_{1j}(t)\times\ldots \\ &\ldots\times H\left(p_{1ij}(\mathrm{t})-\varepsilon_{1ij}(t)\right)\left[y_{ij}(t)-\ldots\right. \\ &\left.\ldots-x_{ij}(t)\right]+c_{2j}r_{2j}(t)H\left(p_{2ij}(t)-\ldots\right. \\ &\left.\ldots-\varepsilon_{2ij}(t)\right)\left[y_j^*(t)-x_{ij}(t)\right]; \end{aligned} \qquad (11)$$

$$\begin{aligned} u_{ij}(t+1) &= w_{2j}u_{ij}(t)+c_{3j}r_{3j}(t)H\times\ldots \\ &\ldots\times\left(p_{3ij}(t)-\varepsilon_{3ij}(t)\right)\left[z_{ij}(t)-\delta_{ij}(t)\right]+\ldots \\ &\ldots+c_{4j}r_{4j}(t)H\left(p_{4ij}(t)-\varepsilon_{4ij}(t)\right)\times\ldots \\ &\ldots\times\left[z_j^*(t)-\delta_{ij}(t)\right]; \end{aligned} \qquad (12)$$

$$\begin{aligned} x_{ij}(t+1) &= x_{ij}(t)+v_{ij}(t+1); \\ g_{ij}(t+1) &= \delta_{ij}(t)+u_{ij}(t+1), \end{aligned} \qquad (13)$$

where $x_{ij}(t)$, $g_{ij}(t)$ and $v_{ij}(t)$, $u_{ij}(t)$ is the position and velocity of i particle of j swarm.

In (11) – (13) $y_{ij}(t)$, $z_{ij}(t)$ and $y_j^*(t)$, $z_j^*(t)$ – the best local and global positions of the i–th particle, found respectively by only one i–th particle and all the particles of j swarm. Moreover, the best local position $y_{ij}(t)$ and the global position $y_j^*(t)$ of the i particle of j swarm are understood in the sense of the first player strategy $x_{ij}(t)$ for minimum of component $\boldsymbol{E}_i(\boldsymbol{X},\boldsymbol{G})$, $\boldsymbol{B_R}(\boldsymbol{X},\boldsymbol{G})$ of the vector payoff (9), (10). However, the best local position $z_{ij}(t)$ and the global position z_j^* of the i particle of j swarm are understood in the sense of the second player strategy $g_{ij}(t)$ for maximum of the same component $\boldsymbol{E}_i(\boldsymbol{X},\boldsymbol{G})$, $\boldsymbol{B_R}(\boldsymbol{X},\boldsymbol{G})$ of the vector payoff (9), (10).

Simulation results. Each naval vessel and each submarine has its own unique signature – a magnetic portrait, which can be used to determine not only the type of technical object, but also this particular technical object. Therefore, the magnetic signatures of specific naval vessel and submarines are a top secret [47, 48].

Measuring the magnetic field signature of naval vessel and submarines is usually carried out when a technical object moves against magnetic field sensors fixedly installed at various points in space. In particular, in the French marine laboratory 13 three-component magnetometers were installed along the body of the technical object being measured [13]. With linear geometric dimensions of a technical object ±100 m and measuring the magnetic field signature after 1 m, the number of measurement points will be 2613 pieces, and the number of measurements will be 7839 values of magnetic field components.

Based on these measurements, a mathematical model of the magnetic field signature is calculated. Recently, moving underwater drones equipped with magnetometers have been used to measure the magnetic signatures of naval vessel and submarines [47, 48].

As an example, consider the magnetic signature of a technical object, the parameters of which are given in [6]. The technical object has linear dimensions from –100 m to +100 m. The initial magnetic field is generated by 16 dipole sources located at points in space of the technical object with the following coordinates. When measuring the magnetic field along the length of a technical object from –100 m to +100 m with an interval of 1 m along three lines with [6] coordinates, 603 measurement points are obtained. In this case, at each point three components of the magnetic field are measured in an orthogonal coordinate system associated with the center of the technical object, so that the total number of measurements is 1809 magnetic field values.

Let us first consider the design of a multyspheroidal model of the initial magnetic field. As a result of solving the predictions of the geometric inverse problem, the coordinates (*x*, *y*, *z*) of the spatial location and their values of the parameters c and the coefficients of the first spheroidal harmonics c_1^0, c_1^1, s_1^1 of 5 spheroidal sources of the multyspheroidal model of the initial magnetic field of the energy-saturated elongated technical object under consideration were calculated by magnetosystems.

1) Sources M_1 – *x* = 24.1775 m, *y* = 0.203945 m, *z* = 1.44653 m, *c* = 17.1245, c_1^0, = –840.073, c_1^1, = 13.9223, s_1^1 = –193.016;

2) Sources M_2 – *x* = –13.2818 m, *y* = 0.498642 m, *z* = 0.266331 m, *c* = 0.232014, c_1^0, = –58875.5, c_1^1, = 1373.1, s_1^1 = –7953.4;

3) Sources M_3 – *x* = –38.496 m, *y* = 0.276427 m, *z* = –1.03295 m, *c* = 0.337585, c_1^0, = –3620.08, c_1^1, = –11852.2, s_1^1 = –3933.69;

4) Sources M_4 – *x* = 241911 m, *y* = 0.203772 m, *z* = 1.4617 m, *c* = 16.9606, c_1^0, = 847.093, c_1^1, = –14.0885, s_1^1 = 194.566.

Figure 2 shows the signatures of the original (solid lines) and model (dashed lines) magnetic field components of the magnetic field for the following coordinate values: *a*) *Y* = –20 m, *Z* = 19 m; *b*) *Y* = 0, *Z* = 19 m; *c*) *Y* = 20 m, *Z* = 19 m; *d*) magnetic field induction modules. As seen in these figures, the signatures of the original and model magnetic fields practically coincide, which confirms the adequacy of the designed multyspheroidal model to the real signatures of the magnetic field.

One of the main technical requirements for the signature of ships and submarines is the limitation of the induction module of the magnetic field signature to the control depth. Technically, it is easiest to compensate for the initial magnetic field using local dipole-type compensators. Let us consider the reduction of the original magnetic field based on the designed multyspheroidal magnetic field model using compensating dipoles.

As a result of solving the control geometric inverse problem of magnetostatics, the spatial location coordinates and values of the magnetic moments of 5 compensating dipoles were calculated

$\{x_1, \ldots, x_5\}$ – {–13.4224, –38.4723, 38.3674, 29.2921, 11.2709} m;

$\{y_1, \ldots, y_5\}$ – {0.557271, 0.2328, –0.886435, –5.39425, 0.341033} m;

$\{z_1, \ldots, z_5\}$ – {0.37837, –1.00586, 0.809621, –1.51659, 0.0348981} m;

$\{M_{x1}, \ldots, M_{x5}\}$ – {1026.93, 136.8, 330.364, 99.726, 468.882} A·m^2;

$\{M_{y1}, \ldots, M_{y5}\}$ – { –48.7259, 900.474, 77.9282, –58.4812, –26.3114} A·m^2;

$\{M_{z1}, \ldots, M_{z5}\}$ – {263.642, 293.553, 135.072, 56.0585, 268.282} A·m^2.

Another technical requirement for the signature of ships and submarines is to limit the amount of change in the horizontal component of the magnetic field at a control depth over a certain period of time when passing a technical object at a given speed.

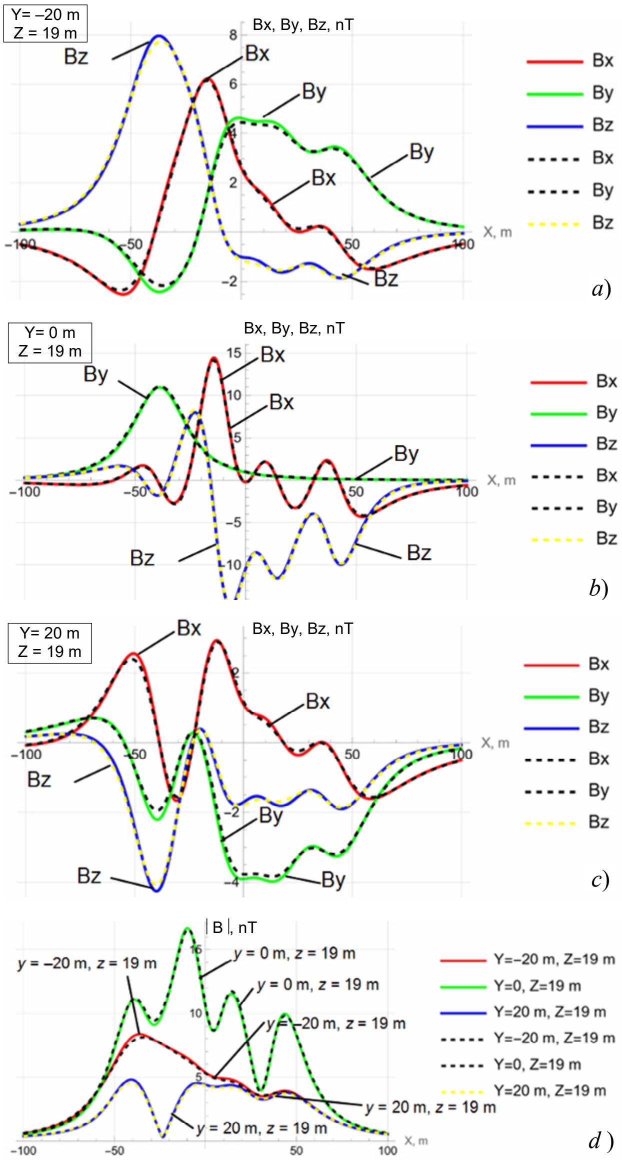

Fig. 2. Signatures of the original (solid lines) and model (dashed lines) magnetic field

Let us now consider the solution of the geometric inverse problem of magnetostatics based on the location of 5 compensation dipoles when introducing into the objective function, in addition to the magnetic field induction modules, also horizontal components at the control depth.

As a result of solving the control geometric inverse problem of magnetostatics, the spatial location coordinates and values of the magnetic moments of 5 compensating dipoles were calculated

$\{x_1, \ldots, x_5\}$ – {11.081, –13.3971, 26.2429, 38.3417, –38.5133} m;

$\{y_1, \ldots, y_5\}$ – {0.148509, 0.547627, –9.81257, –0.832418, 0.288649} m;

$\{z_1, \ldots, z_5\}$ – {0.0697367, 0.302065, –2.47162, 0.512463, –1.01949} m;

$\{M_{x1}, \ldots, M_{x5}\}$ – {469.602, 1040.86, 84.7869, 347.086, 138.088} A·m^2;

$\{M_{y1}, \ldots, M_{y5}\}$ – {–37.4432, –50.1551, –22.2874, 59.2771, 904.151} A·m^2;

$\{M_{z1}, \ldots, M_{z5}\}$ – {252.922, 269.704, 30.4981, 164.38, 298.216} A·m^2.

Figure 3 shows the signatures of the modules: *a*) the initial and resulting magnetic field compensated using 5 dipole sources; *b*) taking into account only the module; *c*) taking into account the horizontal component of the resulting magnetic field at the control depth. The signatures are given for the following coordinate values: *a*) $Y = –20$ m, $Z = 19$ m; *b*) $Y = 0$, $Z = 19$ m; *c*) $Y = 20$ m, Z=19 m.

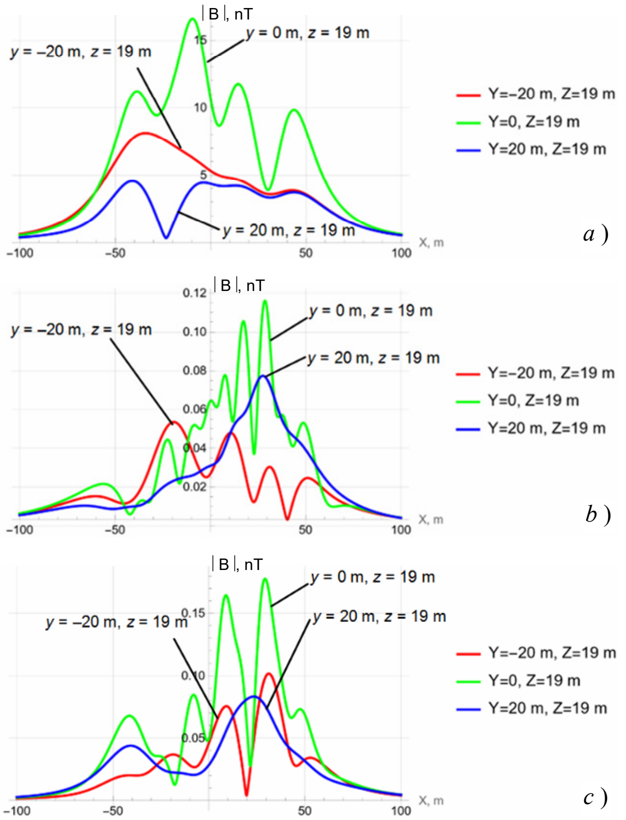

Fig. 3. Signatures of the modules of the initial and resulting magnetic fields

From a comparison of the signatures of the induction modules of the original magnetic field shown in Fig. 3,*a* and the resulting magnetic field shown in Fig. 3,*b*, it follows that with the help of 5 compensation dipoles it was possible to reduce the induction modulus of the original magnetic field by almost 100 times. Taking into account the horizontal component leads to a certain increase in the modulus of the resulting field, as follows from a comparison of Fig. 3,*b* and Fig. 3,*c*.

Figure 4 shows the signatures of the horizontal components of the induction of: *a*) the initial and resulting magnetic field using 5 compensating dipoles; *b*) taking into account only the module; *c*) taking into account the horizontal component of the resulting magnetic field at the control depth.

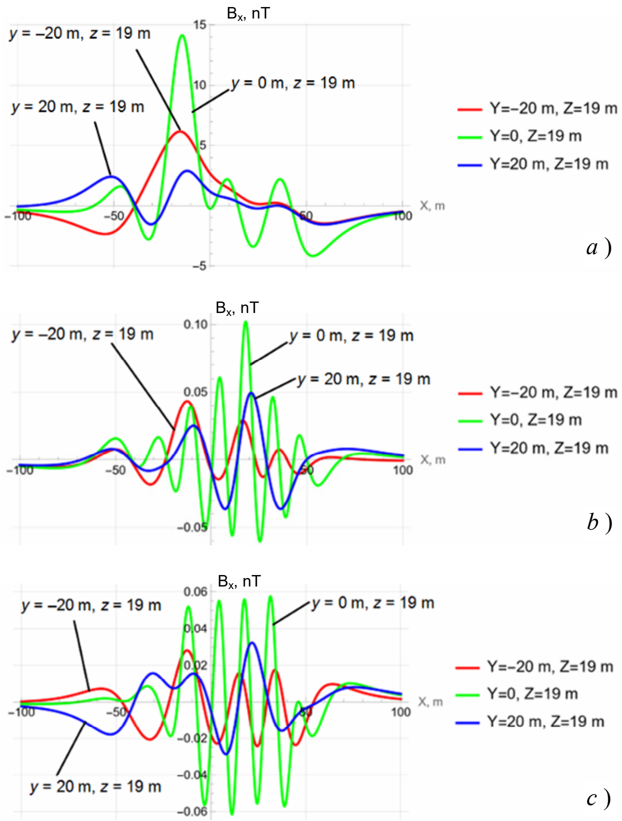

Fig. 4. Signatures of the horizontal components of the initial and resulting magnetic fields

From a comparison of these signatures it follows that with the help of 5 compensation dipoles it was also possible to reduce the horizontal component of the induction of the original magnetic field by almost 100 times. Moreover, taking into account the horizontal component of the magnetic field leads to an additional reduction in the horizontal component of the resulting field by approximately 1.5 times, as follows from a comparison of Fig. 4,*b* and Fig. 4,*c*.

Figure 5 shows the signatures of the longitudinal components of the induction of: *a*) the initial and resulting magnetic field using 5 compensating dipoles; *b*) taking into account only the module; *c*) taking into account the horizontal component of the resulting magnetic field at the control depth.

From a comparison of the signatures of the longitudinal components of the induction of the original magnetic field, shown in Fig. 5,*a* and the resulting magnetic field shown in Fig. 5,*b*, it follows that with the help of 5 compensation dipoles it was possible to simultaneously reduce the longitudinal components of the induction of the original magnetic field by almost 200 times. However, taking into account the horizontal component in the optimization criterion leads to an increase in the longitudinal components of the induction of the resulting field by more than two times, as follows from a comparison of Fig. 5,*b* and Fig. 5,*c*.

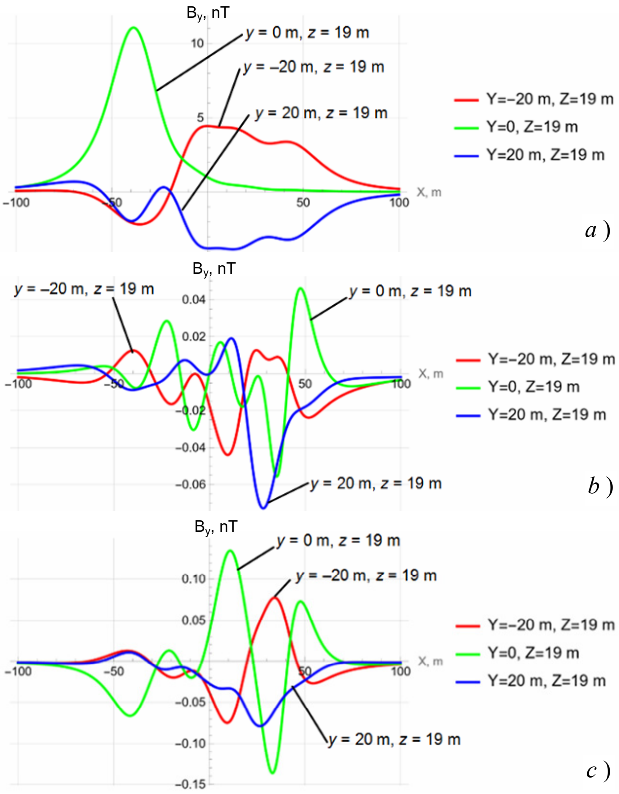

Fig. 5. Signatures of the longitudinal components of the initial and resulting magnetic fields

Figure 6 shows the signatures of the vertical components of induction: *a*) of the initial and resulting magnetic field using 5 compensating dipoles; *b*) when taking into account only the module; *c*) when taking into account the horizontal component of the resulting magnetic field at the control depth.

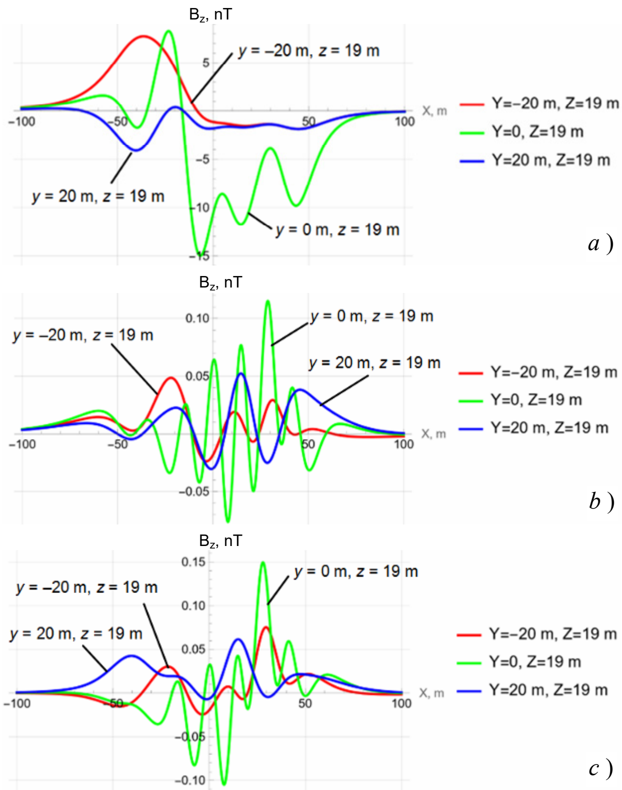

Fig. 6. Signatures of the vertical components of the initial and resulting magnetic fields

From a comparison of the signatures of the vertical components of the induction of the original magnetic field, shown in Fig. 6,*a* and the resulting magnetic field shown in Fig. 6,*b*, it follows that with the help of 5 compensation dipoles it was possible to simultaneously reduce the vertical components of the induction of the original magnetic field by almost 50 times. However, taking into account the horizontal component in the optimization criterion leads to an increase in the vertical components of the induction of the resulting field by more than 1.5 times, as follows from a comparison of Fig. 6,*b* and Fig. 6,*c*.

Thus, by minimizing the magnetic induction modules, a decrease in the module of the resulting magnetic field by more than 100 times is achieved, while simultaneously reducing the magnetic induction components of the resulting magnetic field, also by approximately 100 times. When simultaneously taking into account in the optimization criteria both the magnetic induction modules and the values of the horizontal components of the magnetic induction of the resulting magnetic field, the value of the horizontal component of the resulting magnetic field is additionally reduced by 1.5 times. However, in this case, the modules of the resulting magnetic field, as well as the longitudinal and vertical components of the magnetic field, increase by approximately 1.5 times.

Conclusions.

1. For the first time the method for reduction of magnetic field of uncertain extended technical objects based on their multyspheroidal model and optimization of parameters of compensating dipoles for compensate of spheroidal harmonics of external magnetic field of technical object. Unlike known methods, the developed method makes it possible to increase the efficiency of magnetic field reduction of uncertain extended technical objects.

2. Parameters of compensating dipole magnetic field sources calculated as magnetostatics geometric inverse problems solution in the form of nonlinear minimax optimization problem based on multyspheroidal model of magnetic field of extended technical objects. Nonlinear objective function calculated as the weighted sum of squared of resulting magnetic field COMSOL Multiphysics software package used. Nonlinear minimax optimization problems solutions calculated based on particle swarm nonlinear optimization algorithms

3. Based on the simulation results it is theoretically shown the possibility to reduce by almost 100 times of modulus of induction and horizontal component of the induction of the original magnetic field of uncertain extended technical objects based on optimization of compensating magnetic dipoles spatial arrangement for compensate of spheroidal harmonics of external magnetic field of technical object using multyspheroidal model of the magnetic field.

4. In the future it is planned to conduct experimental studies of the effectiveness of reducing of magnetic field of uncertain extended technical objects based on developed method.

Conflict of interest. The authors declare that they have no conflicts of interest.

REFERENCES

1. Rozov V.Yu., Getman A.V., Petrov S.V., Erisov A.V., Melanchenko A.G., Khoroshilov V.S., Schmidt I.R Spacecraft magnetism. *Technical Electrodynamics. Thematic issue «Problems of modern electrical engineering»*, 2010, part 2, pp. 144-147. (Rus).

2. *ECSS-E-HB-20-07A. Space engineering: Electromagnetic compatibility hand-book. ESA-ESTEC. Requirements & Standards Division*. Noordwijk, Netherlands, 2012. 228 p.

3. Droughts S.A., Fedorov O.P. Space project Ionosat-Micro. Monograph. Kyiv, Akademperiodika Publ., 2013. 218 p. (Rus).

4. Holmes J.J. *Exploitation of A Ship's Magnetic Field Signatures*. Springer Cham, 2006. 67 p. doi: https://doi.org/10.1007/978-3-031-01693-6.

5. Woloszyn M., Jankowski P. Simulation of ship's deperming process using Opera 3D. 2017 18th International Symposium on Electromagnetic Fields in Mechatronics, Electrical and Electronic Engineering (ISEF) Book of Abstracts, 2017, pp. 1-2. doi: https://doi.org/10.1109/ISEF.2017.8090680.

6. Birsan M., Holtham P., Carmen. Using global optimisation techniques to solve the inverse problem for the computation of the static magnetic signature of ships. *Defense Research Establishment Atlantic*, 9 Grove St., PO Box 1012, Dartmouth, Nova Scotia, B2Y 3Z7, Canada.

7. Zuo C., Ma M., Pan Y., Li M., Yan H., Wang J., Geng P., Ouyang J. Multi-objective optimization design method of naval vessels degaussing coils. *Proceedings of SPIE - The International Society for Optical Engineering*, 2022, vol. 12506, art. no. 125060J. doi: https://doi.org/10.1117/12.2662888.

8. Baranov M.I., Rozov V.Y., Sokol Y.I. To the 100th anniversary of the National Academy of Sciences of Ukraine – the cradle of domestic science and technology. *Electrical Engineering & Electromechanics*, 2018, no. 5, pp. 3-11. doi: https://doi.org/10.20998/2074-272X.2018.5.01.

9. Rozov V.Y. *External magnetic fields of power electrical equipment and methods for reducing them*. Kiev, The Institute of Electrodynamics Publ., 1995, no.772. 42 p. (Rus).

10. Rozov V.Yu. Methods for reducing external magnetic fields of energy-saturated objects. *Technical Electrodynamics*, 2001, no. 1, pp. 16-20.

11. Rozov V.Yu. Selective compensation of spatial harmonics of the magnetic field of energy-saturated objects. *Technical Electrodynamics*, 2002, no. 1, pp. 8-13. (Rus).

12. Rozov V.Yu., Dobrodeev P.N., Volokhov S.A. Multipole model of a technical object and its magnetic center. *Technical Electrodynamics*, 2008, no. 2, pp. 3-8. (Rus).

13. Rozov V.Yu., Getman A.V., Kildishev A.V. Spatial harmonic analysis of the external magnetic field of extended objects in a prolate spheroidal coordinate system. *Technical Electrodynamics*, 1999, no. 1, pp. 7-11. (Rus).

14. Rozov V.Yu. Mathematical model of electrical equipment as a source of external magnetic field. *Technical Electrodynamics*, 1995, no. 2, pp. 3-7. (Rus).

15. Volokhov S.A., Dobrodeev P.N., Ivleva L.F. Spatial harmonic analysis of the external magnetic field of a technical object. *Technical Electrodynamics*, 1996, no. 2, pp. 3-8. (Rus).

16. Getman A.V. *Analysis and synthesis of the magnetic field structure of technical objects on the basis of spatial harmonics*. Dissertation thesis for the degree of Doctor of Technical Sciences. Kharkiv, 2018. 43 p. (Ukr).

17. Xiao C., Xiao C., Li G. Modeling the ship degaussing coil's effect based on magnetization method. *Communications in Computer and Information Science*, 2012, vol. 289, pp. 62-69. doi: https://doi.org/10.1007/978-3-642-31968-6_8.

18. Wołoszyn M., Jankowski P. Ship's de-perming process using coils lying on seabed. *Metrology and Measurement Systems*, 2019, vol. 26, no. 3, pp. 569-579. doi: https://doi.org/10.24425/mms.2019.129582.

19. Fan J., Zhao W., Liu S., Zhu Z. Summary of ship comprehensive degaussing. *Journal of Physics: Conference Series*, 2021, vol. 1827, no. 1, art. no. 012014. doi: https://doi.org/10.1088/1742-6596/1827/1/012014.

20. Getman A.V. Spatial harmonic analysis of the magnetic field of the sensor of the neutral plasma component. *Eastern European Journal of Advanced Technologies*, 2010, vol. 6, no. 5(48), pp. 35-38. doi: https://doi.org/10.15587/1729-4061.2010.3326.

21. Getman A. Ensuring the Magnetic Compatibility of Electronic Components of Small Spacecraft. *2022 IEEE 3rd KhPI Week on Advanced Technology (KhPIWeek)*, 2022, no. 1-4. doi: https://doi.org/10.1109/KhPIWeek57572.2022.9916339.

22. Acuña M.H. *The design, construction and test of magnetically clean spacecraft – a practical guide*. NASA/GSFC internal report. 2004.

23. Junge A., Marliani F. Prediction of DC magnetic fields for magnetic cleanliness on spacecraft. *2011 IEEE International Symposium on Electromagnetic Compatibility*, 2011, pp. 834-839. doi: https://doi.org/10.1109/ISEMC.2011.6038424.

24. Lynn G.E., Hurt J.G., Harriger K.A. Magnetic control of satellite attitude. *IEEE Transactions on Communication and Electronics*, 1964, vol. 83, no. 74, pp. 570-575. doi: https://doi.org/10.1109/TCOME.1964.6539511.

25. Junge A., Trougnou L., Carrubba E. Measurement of Induced Equivalent Magnetic Dipole Moments for Spacecraft Units and Components. *Proceedings ESA Workshop Aerospace EMC 2009 ESA WPP-299*, 2009, vol. 4, no. 2, pp. 131-140.

26. Mehlem K., Wiegand A. Magnetostatic cleanliness of spacecraft. *2010 Asia-Pacific International Symposium on Electromagnetic Compatibility*, 2010, pp. 936-944. doi: https://doi.org/10.1109/APEMC.2010.5475692.

27. Messidoro P., Braghin M., Grande M. Magnetic cleanliness verification approach on tethered satellite. *16th Space Simulation Conference: Confirming Spaceworthiness into the Next Millennium*, 1991, pp. 415-434.

28. Mehlem K., Narvaez P. Magnetostatic cleanliness of the radioisotope thermoelectric generators (RTGs) of Cassini. *1999 IEEE International Symposium on Electromagnetic Compatability*, 1999, vol. 2, pp. 899-904. doi: https://doi.org/10.1109/ISEMC.1999.810175.

29. Eichhorn W.L. *Magnetic dipole moment determination by near-field analysis*. Goddard Space Flight Center. Washington, D.C., National Aeronautics and Space Administration, 1972. NASA technical note, D 6685. 87 p.

30. Matsushima M., Tsunakawa H., Iijima Y., Nakazawa S., Matsuoka A., Ikegami S., Ishikawa T., Shibuya H., Shimizu H., Takahashi F. Magnetic Cleanliness Program Under Control of Electromagnetic Compatibility for the SELENE (Kaguya) Spacecraft. *Space Science Reviews*, 2010, vol. 154, no. 1-4, pp. 253-264. doi: https://doi.org/10.1007/s11214-010-9655-x.

31. Boghosian M., Narvaez P., Herman R. Magnetic testing, and modeling, simulation and analysis for space applications. *2013 IEEE International Symposium on Electromagnetic Compatibility*, 2013, pp. 265-270. doi: https://doi.org/10.1109/ISEMC.2013.6670421.

32. Mehlem K. Multiple magnetic dipole modeling and field prediction of satellites. *IEEE Transactions on Magnetics*, 1978, vol. 14, no. 5, pp. 1064-1071. doi: https://doi.org/10.1109/TMAG.1978.1059983.

33. Thomsen P.L., Hansen F. Danish Ørsted Mission In-Orbit Experiences and Status of The Danish Small Satellite Programme. *Annual AIAA/USU Conference on Small Satellites*, 1999, pp. SSC99-I–8.

34. Kapsalis N.C., Kakarakis S.-D.J., Capsalis C.N. Prediction of multiple magnetic dipole model parameters from near field measurements employing stochastic algorithms. *Progress In Electromagnetics Research Letters*, 2012, vol. 34, pp. 111-122. doi: https://doi.org/10.2528/PIERL12030905.

35. Solomentsev O., Zaliskyi M., Averyanova Y., Ostroumov I., Kuzmenko N., Sushchenko O., Kuznetsov B., Nikitina T., Tserne E., Pavlikov V., Zhyla S., Dergachov K., Havrylenko O., Popov A., Volosyuk V., Ruzhentsev N., Shmatko O. Method of Optimal Threshold Calculation in Case of Radio Equipment Maintenance. *Data Science and Security. Lecture Notes in Networks and Systems*, 2022, vol. 462, pp. 69-79. doi: https://doi.org/10.1007/978-981-19-2211-4_6.
36. Ruzhentsev N., Zhyla S., Pavlikov V., Volosyuk V., Tserne E., Popov A., Shmatko O., Ostroumov I., Kuzmenko N., Dergachov K., Sushchenko O., Averyanova Y., Zaliskyi M., Solomentsev O., Havrylenko O., Kuznetsov B., Nikitina T. Radio-Heat Contrasts of UAVs and Their Weather Variability at 12 GHz, 20 GHz, 34 GHz, and 94 GHz Frequencies. *ECTI Transactions on Electrical Engineering, Electronics, and Communications*, 2022, vol. 20, no. 2, pp. 163-173. doi: https://doi.org/10.37936/ecti-eec.2022202.246878.
37. Havrylenko O., Dergachov K., Pavlikov V., Zhyla S., Shmatko O., Ruzhentsev N., Popov A., Volosyuk V., Tserne E., Zaliskyi M., Solomentsev O., Ostroumov I., Sushchenko O., Averyanova Y., Kuzmenko N., Nikitina T., Kuznetsov B. Decision Support System Based on the ELECTRE Method. *Data Science and Security. Lecture Notes in Networks and Systems*, 2022, vol. 462, pp. 295-304. doi: https://doi.org/10.1007/978-981-19-2211-4_26.
38. Shmatko O., Volosyuk V., Zhyla S., Pavlikov V., Ruzhentsev N., Tserne E., Popov A., Ostroumov I., Kuzmenko N., Dergachov K., Sushchenko O., Averyanova Y., Zaliskyi M., Solomentsev O., Havrylenko O., Kuznetsov B., Nikitina T. Synthesis of the optimal algorithm and structure of contactless optical device for estimating the parameters of statistically uneven surfaces. *Radioelectronic and Computer Systems*, 2021, no. 4, pp. 199-213. doi: https://doi.org/10.32620/reks.2021.4.16.
39. Volosyuk V., Zhyla S., Pavlikov V., Ruzhentsev N., Tserne E., Popov A., Shmatko O., Dergachov K., Havrylenko O., Ostroumov I., Kuzmenko N., Sushchenko O., Averyanova Yu., Zaliskyi M., Solomentsev O., Kuznetsov B., Nikitina T. Optimal Method for Polarization Selection of Stationary Objects Against the Background of the Earth's Surface. *International Journal of Electronics and Telecommunications*, 2022, vol. 68, no. 1, pp. 83-89. doi: https://doi.org/10.24425/ijet.2022.139852.
40. Zhyla S., Volosyuk V., Pavlikov V., Ruzhentsev N., Tserne E., Popov A., Shmatko O., Havrylenko O., Kuzmenko N., Dergachov K., Averyanova Y., Sushchenko O., Zaliskyi M., Solomentsev O., Ostroumov I., Kuznetsov B., Nikitina T. Practical imaging algorithms in ultra-wideband radar systems using active aperture synthesis and stochastic probing signals. *Radioelectronic and Computer Systems*, 2023, no. 1, pp. 55-76. doi: https://doi.org/10.32620/reks.2023.1.05.
41. Maksymenko-Sheiko K.V., Sheiko T.I., Lisin D.O., Petrenko N.D. Mathematical and Computer Modeling of the Forms of Multi-Zone Fuel Elements with Plates. *Journal of Mechanical Engineering*, 2022, vol. 25, no. 4, pp. 32-38. doi: https://doi.org/10.15407/pmach2022.04.032.
42. Hontarovskyi P.P., Smetankina N.V., Ugrimov S.V., Garmash N.H., Melezhyk I.I. Computational Studies of the Thermal Stress State of Multilayer Glazing with Electric Heating. *Journal of Mechanical Engineering*, 2022, vol. 25, no. 1, pp. 14-21. doi: https://doi.org/10.15407/pmach2022.02.014.
43. Kostikov A.O., Zevin L.I., Krol H.H., Vorontsova A.L. The Optimal Correcting the Power Value of a Nuclear Power Plant Power Unit Reactor in the Event of Equipment Failures. *Journal of Mechanical Engineering*, 2022, vol. 25, no. 3, pp. 40-45. doi: https://doi.org/10.15407/pmach2022.03.040.
44. Rusanov A.V., Subotin V.H., Khoryev O.M., Bykov Y.A., Korotaiev P.O., Ahibalov Y.S. Effect of 3D Shape of Pump-Turbine Runner Blade on Flow Characteristics in Turbine Mode. *Journal of Mechanical Engineering*, 2022, vol. 25, no. 4, pp. 6-14. doi: https://doi.org/10.15407/pmach2022.04.006.
45. Sushchenko O., Averyanova Y., Ostroumov I., Kuzmenko N., Zaliskyi M., Solomentsev O., Kuznetsov B., Nikitina T., Havrylenko O., Popov A., Volosyuk V., Shmatko O., Ruzhentsev N., Zhyla S., Pavlikov V., Dergachov K., Tserne E. Algorithms for Design of Robust Stabilization Systems. *Computational Science and Its Applications – ICCSA 2022. ICCSA 2022. Lecture Notes in Computer Science*, 2022, vol. 13375, pp. 198-213. doi: https://doi.org/10.1007/978-3-031-10522-7_15.
46. Zhyla S., Volosyuk V., Pavlikov V., Ruzhentsev N., Tserne E., Popov A., Shmatko O., Havrylenko O., Kuzmenko N., Dergachov K., Averyanova Y., Sushchenko O., Zaliskyi M., Solomentsev O., Ostroumov I., Kuznetsov B., Nikitina T. Statistical synthesis of aerospace radars structure with optimal spatio-temporal signal processing, extended observation area and high spatial resolution. *Radioelectronic and Computer Systems*, 2022, no. 1, pp. 178-194. doi: https://doi.org/10.32620/reks.2022.1.14.
47. Wang D., Yu Q. Review on the development of numerical methods for magnetic field calculation of ships. *Ships Science and Technology*, 2014, vol. 36, no. 3, pp. 1-6.
48. Jin H., Wang H., Zhuang Z. A New Simple Method to Design Degaussing Coils Using Magnetic Dipoles. *Journal of Marine Science and Engineering*, 2022, vol. 10, no. 10, art. no. 1495. doi: https://doi.org/10.3390/jmse10101495.

Received 16.05.2024
Accepted 18.09.2024
Published 02.03.2025

B.I. Kuznetsov[1], *Doctor of Technical Science, Professor,*
T.B. Nikitina[2], *Doctor of Technical Science, Professor,*
I.V. Bovdui[1], *PhD, Senior Research Scientist,*
K.V. Chunikhin[1], *PhD, Senior Research Scientist,*
V.V. Kolomiets[2], *PhD, Assistant Professor,*
B.B. Kobylianskyi[2], *PhD, Assistant Professor,*
[1] Anatolii Pidhornyi Institute of Power Machines and Systems of the National Academy of Sciences of Ukraine,
2/10, Komunalnykiv Str., Kharkiv, 61046, Ukraine,
e-mail: kuznetsov.boris.i@gmail.com (Corresponding Author)
[2] Bakhmut Education Research and Professional Pedagogical Institute V.N. Karazin Kharkiv National University,
9a, Nosakov Str., Bakhmut, Donetsk Region, 84511, Ukraine.

How to cite this article:
Kuznetsov B.I., Nikitina T.B., Bovdui I.V., Chunikhin K.V., Kolomiets V.V., Kobylianskyi B.B. Method for reduction of magnetic field of uncertain extended technical objects based on their multyspheroidal model and compensating magnetic dipoles. *Electrical Engineering & Electromechanics*, 2025, no. 2, pp. 48-58. doi: https://doi.org/10.20998/2074-272X.2025.2.07